RESOLUTION PERFORMANCE IMPROVEMENTS IN STARING IMAGING SYSTEMS USING MICRO-SCANNING AND A RETICULATED, SELECTABLE FILL FACTOR InSb FPA

February 1999

Mark E. Greiner, Mike Davis, and John G. Sanders
Cincinnati Electronics Corporation
Mason, Ohio 45040

ABSTRACT

As staring focal plane array (FPA) detectors continue to mature, FPA based IR imaging systems are available in more compact packages that are lighter and consume less power than first or second generation scanning IR sensor packages. However, standard IR analysis models indicate that staring FPA based cameras, while having excellent sensitivity, will have reduced resolution when compared to scanning systems with similar sized detector elements and optics. This apparent resolution limitation is created by the fixed sampling of the active pixel size native to staring FPA systems. Micro-scanning, a technique which moves the image in sub-pixel steps on the focal plane, can provide some over-sampling and reduce this limitation. Standard attempts at micro-scanning using 2-dimensional starring arrays with near 100% fill factor produce only marginal improvements in resolution in these systems. We will present here a new concept in micro-scanning using an InSb FPA with reticulated detector elements and active area masking to provide a well defined, selectable fill factor.

A compact micro-scanned imaging system design that weighs less than 8 pounds and consumes less than 15 watts is presented here. MRTD (Minimum Resolvable Temperature Difference) analyses demonstrating a 2X improvement in resolution in both vertical and horizontal directions over non-micro-scanned systems has been measured, a performance level which micro-scanned systems with non-reticulated FPAs cannot approach. Test data from this system will also be presented including NETD and MRTD performance.

1.0 INTRODUCTION

In the last decade, Staring Focal Plan Array (FPA) based thermal imagers have shown a steady increase in performance – in resolution, sensitivity, compactness of package, low power and in overall picture quality. Yet, every increase in performance is absorbed by the system user with a demand for even greater performance in the next iteration of camera design. Today, most of the improved system performance comes with the need for larger arrays, larger substrates and larger dewar/cooler/array assemblies – at the cost of a more expensive array and a higher power cooler.

In 1997, Cincinnati Electronics Corp. (CE) developed a compact, low-cost, general purpose, MWIR imager and demonstrated a significant improvement in most areas of system performance. Called the NightConqueror system, this compact, multipurpose thermal imaging sensor is capable of displaying images from many formats of focal plane array (FPA) detectors. The system can display images from high density 640 x 512 pixel FPAs, medium density 256 x 256 or 320 x 240 pixel FPAs, or one or two axis micro-scanned medium density FPAs.

In 1998 CE designed and manufactured a front-side illuminated, 100% reticulated, low fill factor (25%), medium density (256 x 256) array FPA to demonstrate the resolution improvement possible with a properly implemented 2-axis dither system. A NightConqueror camera was used to implement the system design. This paper

Form SF298 Citation Data

Report Date *("DD MON YYYY")* 00021999	**Report Type** N/A	**Dates Covered (from... to)** *("DD MON YYYY")*

Title and Subtitle Resolution Performance Improvements in Staring Imaging Systems Using Micro-Scanning and a Reticulated, Selectable Fill Factor InSb FPA	**Contract or Grant Number**
	Program Element Number
Authors	**Project Number**
	Task Number
	Work Unit Number
Performing Organization Name(s) and Address(es) Cincinnati Electronics Corporation Mason, Ohio 45040	**Performing Organization Number(s)**
Sponsoring/Monitoring Agency Name(s) and Address(es)	**Monitoring Agency Acronym**
	Monitoring Agency Report Number(s)
Distribution/Availability Statement Approved for public release, distribution unlimited	
Supplementary Notes	
Abstract	
Subject Terms	
Document Classification unclassified	**Classification of SF298** unclassified
Classification of Abstract unclassified	**Limitation of Abstract** unlimited
Number of Pages 15	

will present information demonstrating how this reticulated, low fill-factor staring FPA construction can generate almost twice the resolution performance of a similar pitch FPA with little loss of sensitivity. This double resolution is a significantly better improvement than previously published methods of using micro-scan for improving the resolution of high-fill factor FPAs. In the following sections, this paper will describe the optical design, FPA design and methods used to create this double resolution performance.

2.0 MICRO-SCANNING – AN OVERVIEW OF PREVIOUS SYSTEMS

The process of micro-scanning involves "scanning" the scene by laying a series of images in fractional pixel steps across the detector array. These partial-images are made into a composite image. Each partial-image is a full field image made at a rate faster than the composite image. The composite image is built at the effective "real time" display rate of the system to maintain a live display. Since the motion between image fields is so small, micro-scanning is often called "dithering" the array. This small motion (dither) scanning process accomplishes two things:

- The micro-scanning technique corrects for the Nyquist sample-limited resolution performance of normal staring arrays and extends the un-aliased resolution performance.

- The motion can create a resolution (Modulation Transfer Function or MTF) increase based on the "less than 100%" fill factor response in the array.

When a staring (unmoving) FPA camera is used to observe a scene that is also not moving there will be a resolution limitation due solely to the sampling lattice . Since the array and scene are not moving, the resolution limit for high frequency scene content will occur at the point where the scene frequency is equivalent to two staring detector element pitches. This is the Nyquist sample-limited resolution performance. When a staring FPA is dithered, the image is shifted in sub-pixel increments and the array is sampled at each shifted location. This has the same effect on correcting for aliasing as the over-sampling of a scanned system.

FPAs may have areas between active detector elements, which are not responsive to scene image (inactive area). The ratio of the active area size to the total array size is the fill factor. Dithering an array with a high fill factor, or a diffuse active area dimension, can show a some improvement in resolution when micro-scanned. However, low fill factor arrays with finely differentiated active areas can show significant resolution increases with micro-scanning. The typical resolution improvement factor for a "100% fill-factor"FPA can be as much as 15% while a 25% fill factor (available in a reticulated, frontside illuminated array) can show as much as four times the resolution (twice the resolution in each axis).

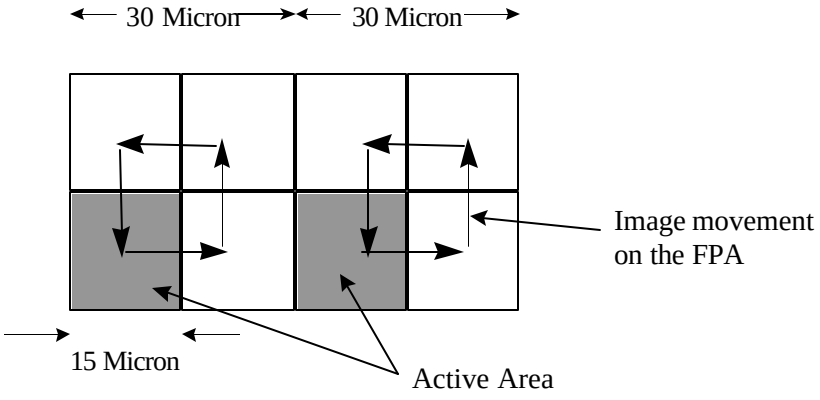

Figure 1. A small reticulated detector area with low fill factor provides high MTF while micro-scanning doubles the sampling rate in both directions.

In a staring array, the optical resolution (diffraction spot size) typically is set to be slightly larger than an active element, creating a smooth image. In a dithered system, the optical resolution of the optic is increased, usually by increasing the aperture (decreasing the f/number) until the spot size encompasses only one element. This would normally leave an image gap between elements, but the micro-scanned system fills in the inter-element areas by micro-scanning through the dead areas. By modifying the optics for higher resolution and dithering the image, the system Nyquist rate is increased. The system MTF is also increased via the smaller pixel active area. Both of these improvements are required to realize a significant increase in system resolution.

3.0 ARRAY CONSTRUCTION AND RESOLUTION

There are two different types of InSb FPA construction with significant differences in their resolution capability[1]. Backside illuminated arrays have a continuous absorbing layer that covers all the pixels. These arrays absorb photons on the back surface away from the P-N junction, followed by photocarrier diffusion to the junction. This carrier diffusion is a random process, occurring laterally to other pixels as well as vertically. This leads to an effective defocusing of the active area in backside illuminated arrays and limits how small the "effective active area" of each element can be made, reducing the overall resolution in micro-scanning operation. This effect can be reduced somewhat by careful thinning of the absorbing layer, but is limited due to the need to absorb all the photons and to maintain a high quality P-N junction. The frontside illuminated, fully reticulated InSb array construction, however, places the P-N junction on the same side as the photon absorption and uses a reticulated, not continuous, absorbing layer. Since a frontside illuminated FPA absorbs photons strongly in the P-N junction region and the absorbing layer is reticulated, no carrier diffusion is possible to adjacent pixels and, therefore, has a higher inherent resolution for micro-scanning. The key difference between the reticulated frontside illuminated array and the backside illuminated array construction is the ability, in the reticulated design, to create a "finely delineated" active area. The dimension of this area is determined by the application of a precisely controlled optically opaque mask. This is shown in Figure 2 for a backside and frontside illuminated cell of identical size, where the detector size is equal to 15 microns. See reference 1 for additional background on these calculations.

For the reticulated InSb FPA used in the micro-scanned system in this paper, the active area was reduced in both dimensions to one-half the detector spacing (see Table 1), creating a focused response of the dimension in Figure 2. Once the active element size is reduced to half its normal size in each axis, a 2-axis micro-scan can be used to reconstruct the display frame with twice the original resolution. Data for this paper was produced in this manner. Figure 3 compares the calculated MTFs vs spatial frequency (f) and folded (aliased) frequencies ($f_s - f$) of reticulated and backside illuminated arrays. Both are 15 micron junctions on 30 micron centers. In both cases micro-scanning has doubled the Nyquist cutoff, however, the MTF for the reticulated array is higher and this allows much fuller signal modulation at the Nyquist cut-off frequency. The result is a higher pixel MTF and lower system MRTD at these extended spatial frequencies, and increased system resolution.

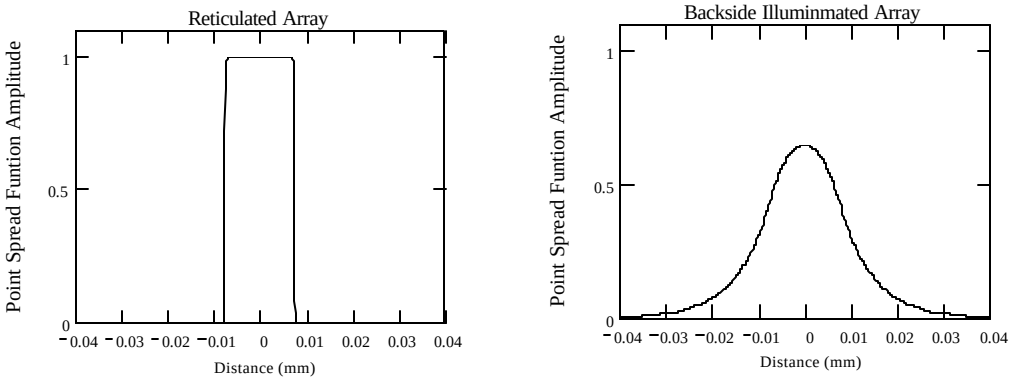

Figure 2. These point spread functions compare resolutions of the reticulated and backside illuminated devices with 15 micron junctions. The bell shaped curve spreading is due to diffusion of photo-generated carriers.

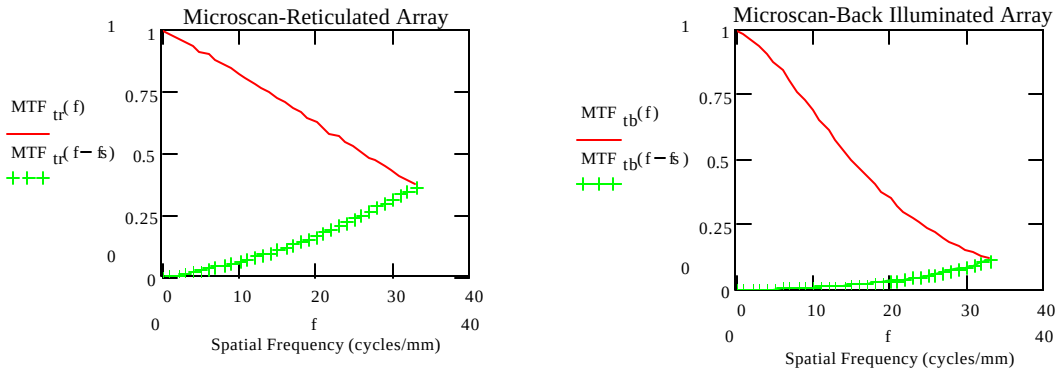

Figure 3. These plots depict the calculated MTFs vs spatial frequency (f) and folded (aliased) frequencies ($f_s - f$) of reticulated and backside illuminated arrays corresponding to the spatial domain of Figure 2. Both MTF calculations include diffraction effects for f/2 optics while the back illuminated MTF includes carrier diffusion effects from reference 1. Note that at the micro-scanned Nyquist frequency, the signal modulation for the reticulated array is calculated to be about 3 times higher than the signal modulation of the backside illuminated array

4.0 THE REAL TIME ISSUE

One problem that must be dealt with in micro-scanned systems is the response of the sensor, which should approach "real-time" video imagery. For the micro-scanning technique to be effective, the micro-scanning must occur at the effective frame rate of the system. The composite image must be built from images taken at "the same time" so that object motion and blurring won't reduce the resolution enhancements or create unacceptable image aberrations such as double images and ghosting. The maximum effective frame rate in an FPA is usually a function of either detector integration time or maximum readout rate of the array.

The quantum efficiency of the array plays a major part in the real time problem. Low quantum efficiency arrays, such as PtSi, must provide integration times of 10 milliseconds to achieve reasonable system sensitivities (0.1°C using f/1.5 optics). High quantum efficiency arrays can easily provide better sensitivity (0.025°C NETD using f/2.0 optics) with less than 5 milliseconds of integration time. The true, real time image display rate of a dithered FPA system will depend on the integration time and the number of dither locations used. A frame integration must be made at each dither location and a composite image created from all dithered partial images before displaying.

The NightConqueror electronics were configured to control, process and display the information from the array. The system frame rate is 30 per second. The total frame time must be divided among the four partial images that create the composite image, so the FPA was read out at a rate of 120 Hz or 8.33 msec per FPA frame. Some time must be allowed for the dither mechanism to settle between movements. For this micro-scanning optic, 1 millisecond was found to be sufficient. This left 7.3 msec for signal integration. For the data presented here, the integration time for each sample (four per frame) was 5.7 milliseconds, a bit under the maximum of 7.3 msec. Because of the ample signal available at the FPA, this integration time was sufficient to provide 0.025°C NETD.

5.0 MICRO-SCAN SYSTEM DESCRIPTION

As was mentioned previously, the detector array for this system is an InSb device with reticulated pixels. The pixels are on 30 micron centers with an active area of 16 X 16 micron. Image motion at the FPA, created by the micro-scanning mechanism of the dithering optic, fills in the gaps. See Figure 1 for a visualization of this action. The dithering mechanism uses a high accuracy dual piezoelectric XY-positioning stage attached to one of the optical elements. Movement of this element in two dimension orthogonal to the optical axis changes the image position at the FPA in both the horizontal and vertical directions.

The optic has an EFL (effective focal length) of 250 mm. The detector/dewar assembly included a f/2 cold shield that provided the exit pupil for the system. At f/2, the diffraction limited Airy disc has a 20 micrometer diameter at the focal plane.

6.0 ANALYSIS OF MICRO-SCANNING PERFORMANCE - A COMPARISON

It is the aim of this section to examine the projected performance of a 256 X 256 format micro-scanned system and compare it to the performance projected for a 256 X 256 format non-micro-scanned system. The analysis is to include a comparison of the projected NETD and MRTD metrics. Table 1 below summarizes some of the fundamental parameters of both systems.

Table 1. This is a summary of some fundamental parameters of the two systems that are analyzed and compared. Note that the fields-of-view of the two systems are the same but the pupil diameter of the micro-scanned system is larger to reduce the spot size for the smaller detector.

	256 X 256 Micro-scan	256 X 256 Staring
Pixel Active Dimension	16 micron	26 micron
Pixel Pitch	30 micron	30 micron
Field-of-View	1.76° X 1.76°	1.76° X 1.76°
Optics Focal Length	250 mm	250 mm
f-number	2	4
Frame Rate	30 Hz	30 Hz
Detector Angular Subtense (DAS)	64 μRad	104 μRad
Nyquist Rate	8.33 cycles/mRad	4.16 cycles/mRad
Airy Disc Diameter	78 μRad	156 μRad
Entrance Pupil Diameter	125 mm	62.5 mm

The pixel pitch for the micro-scanned detector is 30 microns, however the reticulated active pixel dimension is 16 micron. Image motion at the FPA by the micro-scan mechanism fills in the spaces with a 2 X 2 dither resulting in an equivalent pitch of 15 micron. An active pixel dimension of 16 microns was chosen to provide a slight amount of oversampling.

The MTF of the optics is estimated by cascading the diffraction limited MTF. This is given by

$$MTF_{opd} = \frac{2}{p}\left[\arccos\left(\frac{f}{f_{oc}}\right) - \left(\frac{f}{f_{oc}}\right) \bullet \sqrt{1-\left(\frac{f}{f_{oc}}\right)^2}\right], \quad (1)$$

with a factor that approximates additional optical aberrations in addition to the diffraction limit[2].

$$MTF_{opab}(f) = 1-\left(\frac{Wrms}{A}\right)^2\left[1-4\left(\frac{f}{f_{oc}}-\frac{1}{2}\right)^2\right] \quad (2)$$

f_{oc} is the optical cutoff frequency and f the spatial frequency. Both have units of cycles/mRad. For the empirical constant $A = 0.18$ and a wave front rms error of $Wrms =$ 1/14, the cascaded result approximates a well-designed real optic. The result is 80-85% of the diffraction limit at one-half the optical cutoff frequency.

The MTF of the reticulated detector pixel is

$$MTF_d(f) = \frac{\sin\left(\frac{p \bullet W \bullet f}{EFL}\right)}{\frac{p \bullet W \bullet f}{EFL}}, \quad (3)$$

where W is the detector pixel active area extent and EFL is the optics focal length. Note that equation (3) is not applicable to backside illuminated arrays. For BSI arrays the detector aperture is not reticulated and is limited by the lateral diffusion of the photo-generated carriers. A detailed analysis of this effect is discussed in reference 1. The Kornfeld and Lawson model[3] is used to model the MTF of the human observer's eye. A high resolution monitor with an MTF of 0.34 at the raster frequency is assumed.

An analysis of system sensitivity (noise equivalent temperature difference or NETD) was performed for the two systems. In this analysis, the integration time for the non-micro-scanned staring system was selected to be 14 milliseconds. At 14 milliseconds the full well capability of the multiplexer (1.2 X 10^7 electrons) is filled when the object temperature is about 45° C. As discussed previously, the signal integration time for the micro-scanned system is limited to 7.3 msec, which may affect system sensitivity. For this analysis, the integration time for the micro-scanned system was selected to be 5.7 msec, which did not completely fill the well capacity of the multiplexer for a 45C background. Because of these set-up conditions, it is then expected that the NETD of the micro-scanned system would be slightly inferior.

The NETD is estimated by the equation

$$NETD(T) = \frac{\sqrt{Nwf(T) + dN_e^2}}{C(T) \bullet Ns(T)}, \quad (4)$$

where $Nwf(T)$ is the total number of charge carriers at the storage site or the total background. It includes estimates of emissions and reflections from imperfect optics ($\tau_{op} < 1$) and detector leakage current, in addition to, the photo-generated carriers caused by the scene. dNe is the noise generated within the readout circuit and processing

electronics. It is estimated to be the equivalent of 1500 electrons. $Ns(T)$ is the number of photo-generated carriers from the image scene mentioned above. It is a function of the scene radiance or temperature T as well as optics transmission, f-number, detector active area, detector quantum efficiency and integration time. $C(T)$ is the relative thermal contrast with $M_p(\lambda, T)$ the Planck spectral photon exitance of a blackbody.

$$C(T) = \frac{\int_{\lambda} \frac{\partial M_p(\lambda, T)}{\partial T} d\lambda}{\int_{\lambda} M_p(\lambda, T) d\lambda} \qquad (5)$$

Figure 4 depicts the NETD estimates for both systems as a function of scene temperature. Note the slightly better performance of the staring array. This is expected because slightly less signal is collected by the micro-scan system. Optics transmission (80%) and detector quantum efficiency (85%) were taken to be the same for both systems.

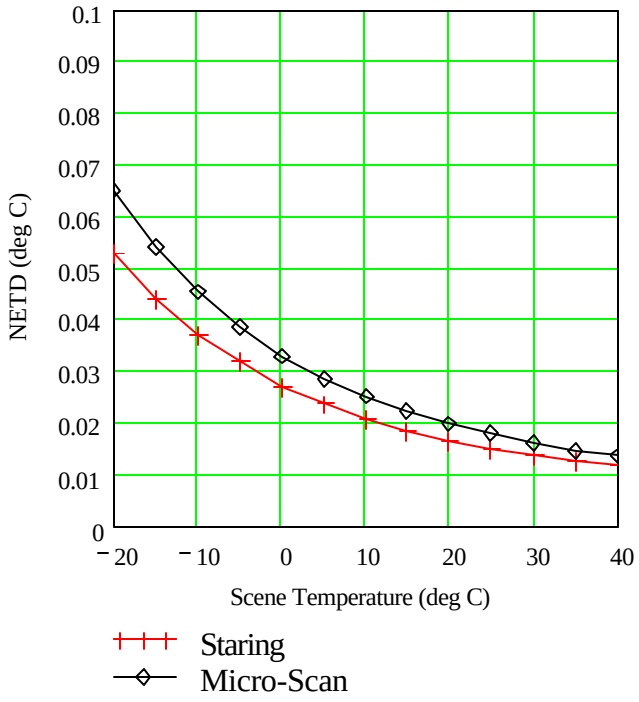

Figure 4. A comparison of the predicted Noise Equivalent Temperature Difference for the two systems. The smaller well fill for the micro-scan system results in a larger NETD.

The Minimum Resolvable Temperature Difference (MRTD) measure takes into account both the sensitivity and resolution or MTF, as well as the performance of the operator. A general form of an MRTD expression is given by equation (6).[4]

$$MRTD(f) = \left(\frac{\frac{p}{8} SNR_{TH} \bullet NETD \bullet k(f)}{MTF(f)} \right) \left[E_t \bullet E_h(f) \bullet E_v(f) \right]^{1/2} \qquad (6)$$

SNR_{TH} is the threshold signal to noise ratio required to recognize the target. $k(f)$ is the system noise correction function. E_t, $E_h(f)$, and $E_v(f)$ are the temporal, horizontal spatial integration, and vertical spatial integration factors of the eye and brain. Figure 5 is a prediction based on equation (6). The MRTD lines stop at the Nyquist frequency of each system; the Nyquist frequency being the highest spatially frequency that can be reproduced. Note that predicted micro-scanned MRTD is nearly identical to the staring system MRTD except that the spatial frequencies are doubled. This result is due to the small increase in NETD in the micro-scanned system, even with four times the sampling and shows that the micro-scanning doubles the system resolution without a significant loss in system sensitivity (note that to achieve this increased resolution, that the size of the optics must be increased to compensate for the smaller detector size). The staring system MRTD at Nyquist is somewhat better than the micro-scanned sytem at it's Nyquist rate because both the NETD and MTF at Nyquist are marginally improved over the micro-scanned device.

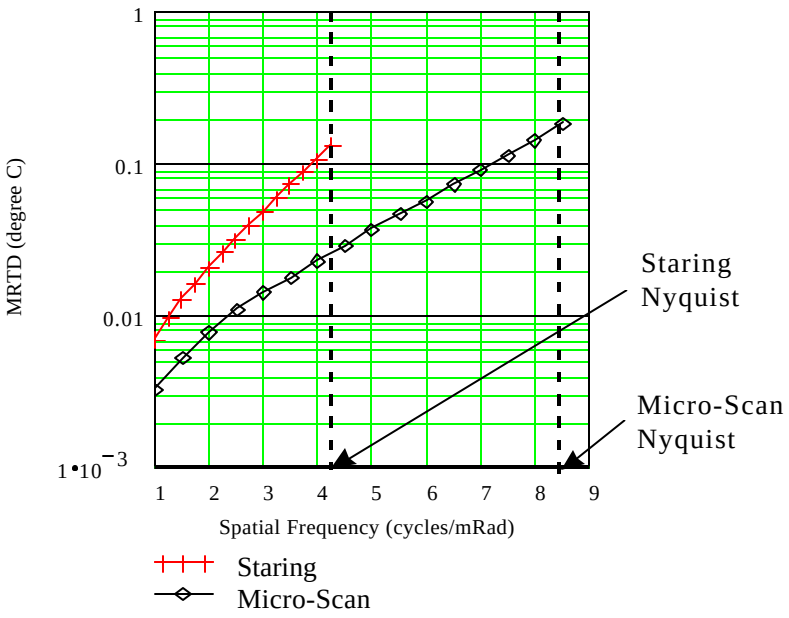

Figure 5. These curves are modeled predictions of the MRTD of both systems and are plotted out to the Nyquist frequency in each case.

7.0 TEST DATA AND COMPARISON WITH THE MODELS

The NETD of the micro-scanned system was measured at four different scene temperatures. The results are shown in Figure 6 along with the prediction that was discussed in the previous section. The test results agree remarkably well with the model's prediction.

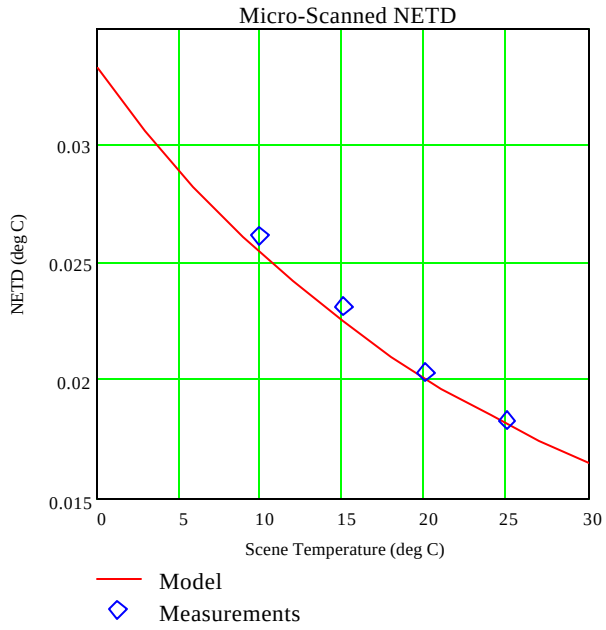

Figure 6. The Noise Equivalent Temperature Difference data agree with the model predictions.

Figure 6 demonstrates that excellent NETDs can be achieved with micro-scan even though less than ¼ the frame time is allowed for signal collection. High quantum efficiency detectors make this performance feasible. The f-number advantage of the micro-scanned system (f/2 versus f/4) results in a higher focal plane irradiance for the smaller pixel area operated at a smaller integration time. The result is NETD performance approaching the staring system. One could argue that it is not appropriate to compare NETD performance between systems with different f-numbers. However, the larger pixels in the staring system do not require f/2 optics and provide sufficient sensitivity for most imaging applications at f/4.

MRTD data were taken for both a 256 X 256 micro-scanned system and a 256 X 256 staring system. A description of the measurement techniques is provided in the appendix. The micro-scan system data is shown in Figure 7 and compared to the predicted MRTD performance with marginal agreement, especially at low frequency. At this time, the source of the discrepancy is not known. The graphed data is the geometrically averaged data of six separate measurements by three different observers. The micro-scanned system data clearly shows that with a pixel pitch of 30 micron and an optic focal length of 250 mm, targets can be resolved out to 8.3 cycles/mRad. Micro-scan has clearly doubled the sampling and Nyquist rates without impacting the system sensitivity.

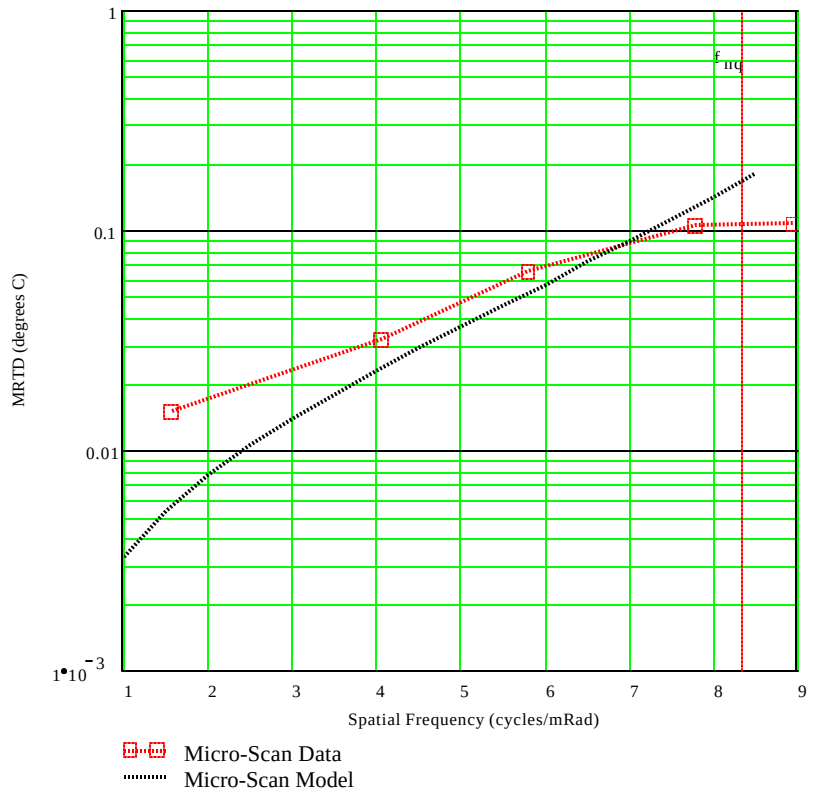

Figure 7. This chart compares the measured MRTD of the micro-scanned system with the performance prediction of Section 6.

Figure 8 shows MRTD measurements for both the micro-scanned and non-micro-scanned systems. When both systems have the same field of view, it is clear that micro-scanning, with its increased Nyquist frequency, can increase system resolution by a factor of two. As expected, though, this increased resolution requires a larger optical entrance aperture. The benefit for micro-scanning is that sensor resolution can be doubled while maintaining the original field-of-view, a benefit similar to upgrading sensors from a 256 x 256 pixel format with f/4, 250mm optics to a 512 x 512 pixel format with f/4, 500mm optic. The micro-scanned system will have an entrance aperture similar to the 512 x 512 optics, as well as comparable resolution.

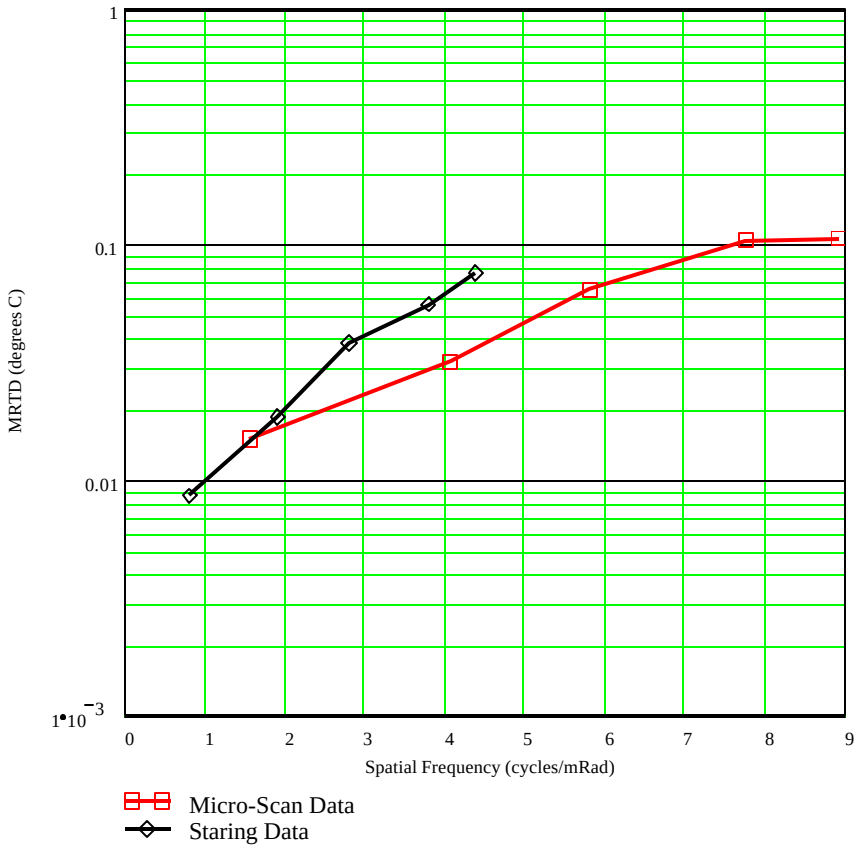

Figure 8. This graph compares the measured MRTDs of the two systems. Micro-scanning has doubled the resolution.

The performances can also be compared by estimates of recognition ranges. These estimates can be made graphically as shown in Figure 9. The spatial frequencies of the MRTD measurements are replotted as range (rescaled to the target discrimination value based on a target size of 2.3 meters and the required 3 cycles on target for recognition). Also plotted is the target-background temperature difference (2°C) and the reduction in target-background temperature difference as a function of range. The crossing of the apparent temperature line with the MRTD line is the maximum range of task performance. In good weather, the target signal is not attenuated below the MRTD limit at Nyquist and the range performance is determined solely by the Nyquist frequency. In this case, micro-scanning doubles the target recognition range from 3.1km to 6.2km. Under limited weather conditions, the target signal is attenuated below the MRTD limit after 3km. Here, micro-scanning only provides a marginal increase in recognition range under limited weather conditions. For wider field-of-view applications, where recognition ranges are under 1.5 km for the staring system, there will be a 2x range improvement in both good and limited weather conditions with micro-scanning.

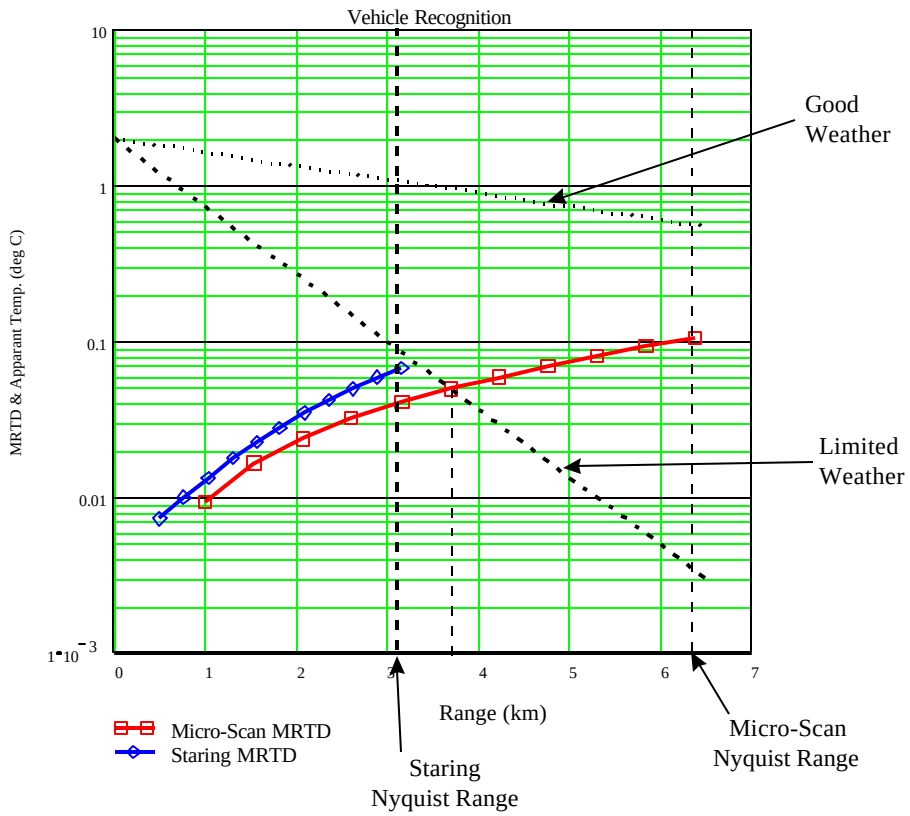

Figure 9. A graphical solution for determining recognition ranges for imaging systems with a field-of-view of 1.8°. The staring system recognition range is resolution limited to 3.2 km for both weather conditions. The micro-scanned system is resolution limited at 6.4 km in good weather and sensitivity limited to about 3.7 with limited weather. Signal extinction coefficients of 0.2/km for good weather and 1.0/km for limited weather were used.

8.0 CONCLUSIONS

The use of high resolution MWIR imaging systems is increasing as high quantum efficiency InSb focal plane arrays find acceptance in many traditionally LWIR or scanning system applications. These MWIR systems are available at a low cost in many “off-the-shelf” configurations. They typically require little power or space and provide excellent sensitivity and resolution. Micro-scanning, when used with a high quantum efficiency focal plane array sensor, can increase system resolution without loss of sensitivity due to the excess signal available to the FPA. When a reticulated, front-side illuminated InSb focal plane array is used in a 2x2 micro-scanned system, and the fill factor is optimized for micro-scanning, a factor of two improvement in resolution in each axis is achieved. In this paper, both performance predictions and initial test results from a micro-scanned system using an array of this type have been presented. Further performance improvements are expected as this system is optimized.

The benefits of micro-scanning a reticulated, front-side illuminated InSb FPA were examined by analyzing the theoretical MTF of the array. These reticulated pixels had superior MTF when compared to backside illuminated pixels with diffusion limited resolution. The primary MTF improvement of frontside illuminated, reticulated arrays over backside illuminated arrays is due to the absence of pixel cross-talk from photocarrier diffusion and the presence of an optically opaque grid on the detector array that precisely defines the sensor active area. The calculated pixel MTF and the system NETD (along with the reduction in pixel size to 16 microns required by micro-scanning) were used to predict the MRTD of the micro-scanned system. These performance improvements expected with a

reticulated array were the primary motivation for fabricating and testing a high resolution micro-scanned system. Initial testing of this system has demonstrated this predicted resolution improvement.

When evaluating the performance of micro-scanned systems, it is desirable to compare systems with the same field-of-view. The data presented has shown that, when systems are compared in this way, the micro-scanned system has a 2X improvement in resolution in both the vertical and horizontal directions and MRTD comparable to a 512 x 512 sensor. This is due to the 2x increase in the system Nyquist spatial frequency without a compromise in signal modulation at these extended spatial frequencies. This effect was evident in the comparison of system MRTD. Note that it is possible to increase the resolution of a pure staring system by increasing the focal length of the optics, but this results in a 2x reduction in system field-of-view, not a desirable trade-off. Micro-scanning provides the system designer an opportunity to increase system resolution while maintaining field-of-view without the high cost of larger format arrays. For resolution requirements beyond a 640 x 480 array, this same technology is available to micro-scan a 640 x 480 FPA, creating an image with 1280 x 960 pixel resolution. In this ultra-high resolution system, though, there will still be significant issues of data transfer rate and display resolution to be resolved.

In most applications, the increased resolution realized by micro-scanning extends the recognition range of FPA based imaging systems. For the FPA based system presented here, there is sufficient sensitivity to resolve the target above the noise. In these cases, recognition ranges are determined by system resolution, not sensitivity, and the micro-scanned system presented here is predicted to have a 2x increase in recognition range over a non-micro-scanned system with the same field-of-view. Even under adverse weather conditions, when atmospheric attenuation reduces the target signal below the system noise limit, some additional recognition range will be realized in the micro-scanned system.

Micro-scanned systems, using reticulated, high quantum efficiency sensor arrays, can provide the system designer an alternative to higher cost, higher density sensor arrays. In addition, where sensor technology does not exist at the required format, system designers can choose to micro-scan state-of-the art sensors to achieve the required system resolution. Using reticulated InSb sensor arrays with a customized fill factor will provide the best resolution performance for systems with micro-scanning requirements.

9.0 ACKNOWLEDGEMENTS

The authors would like to acknowledge Jim Howard at Telic OSTI for the design and manufacture of the micro-scanned optics, Ed Brinkman, Dave Grebe, Dick Karaus for support of the microscanning electronics requirements, and Chuck Martin and Rich Rawe for providing the reduced fill factor reticulated InSb FPA .

Appendix A – MRTD Measurements Methodology

Following is a summary of the MRTD methods used in this paper. MRTD is defined as the lowest target to background temperature difference at which a standard test pattern can be resolved by an observer. The standard test pattern is a four bar chart with a 7:1 aspect ratio. During the test, the observer either increases or decreases the temperature difference between the source and the background until all four bars of the test target are just visible. The temperature difference is recorded as the MRTD at the frequency of the test target. MRTD is generally a function of the background temperature and orientation of the target. Normally, the background temperature cannot be controlled, but it is recorded during the tests.

During the tests the operator is allowed to optimize his viewing conditions and adjust any settings or controls on the imager under test. He may alter the illumination in the room and adjust the viewing distance. He may also slightly adjust the position of the target within the field of view. The following have been established as minimum measurement conditions:

1) The emissivities of the test pattern and the blackbody must be at least 0.95.
2) The spatial frequencies must be within 5% of the values stated as nominal.
3) The blackbody and controller must have the capability of setting the temperature difference to a resolution of at least 0.001 degrees C.
4) Any variation in temperature across the useful area of the test target is so small as not to be detectable by the observer
5) The transmission losses between the imager and the test target should be known and taken into account when the data are reduced.
6)At any time during the measurement the observer may optimize the controls on the imager, adjust the illumination the illumination level in the laboratory, optimize the viewing distance or change the position of the pattern within the field of view.
7) The monitor is set up for optimum viewing at the beginning of the test and not adjusted during the measurements.
8) Measurements are taken at a minimum of four spatial frequencies. The lowest frequency chart should be from 10% to 25% of the Nyquist frequency. The two highest frequency charts should be just below and just above the Nyquist rate.
9) Measurements start using the lowest spatial frequency target progressing to the higher frequency bars.
10) Three or more observers are used and the results geometrically averaged.

Due to the limitations of the test equipment, the temperature difference indicated by the temperature controller may not be the true temperature difference between the blackbody and the test pattern. To cancel out any offset in temperature readings, the following 2 step process is followed. The observer starts with a temperature difference where the target is not visible and increases the temperature until the target is just resolved. That temperature difference is ΔT_{plus}. Again starting with a temperature difference where the target is not visible, the operator decreases the temperature until the target is just resolved. That temperature difference is $\Delta T_{\min us}$. The MRTD is then

$$\left(\frac{\Delta T_{plus} - \Delta T_{\min us}}{2}\right) \bullet \mathrm{T}_{col}, \qquad (5.1)$$

where T_{col} is the total collimator transmittance.

The collimator transmittance is measured by comparing the response of a system on the collimator to the response of the of the system without the collimator. The measurement without the collimator is taken at a distance from the blackbody equal to the collimator focal length plus the distance from the collimator main mirror to the system. The infrared system used for this measurement must have the same spectral response as the system under MRTD test. The two data sets are plotted versus calculated blackbody exitance and least squares fit to straight lines.

The ratio of the slopes of the two fits is the collimator transmittance. Figure A.1 shows the results of a collimator transmittance measurement using an imager with the same spectral response as the systems discussed in this paper. The result is a transmittance of 0.937.

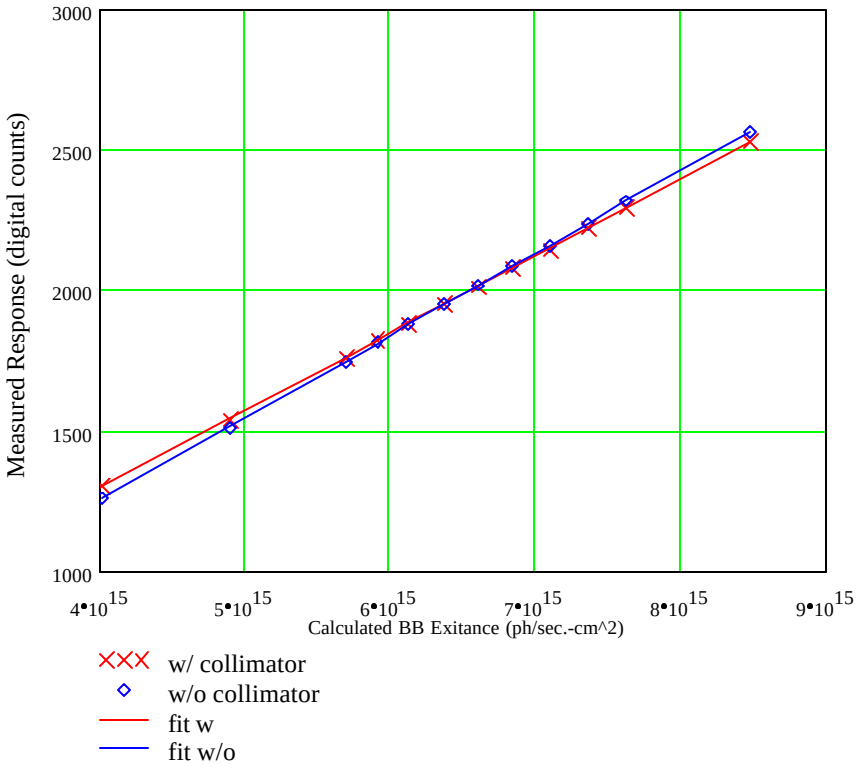

Figure A.1. The ratio of the slopes of the lines is the collimator transmittance. The lines are determined by measuring system response with the collimator and without the collimator at the same distance from the source. The transmittance resulting from this measurement is $T_{col} = 0.937$.

---

[1] M. Davis, M. Greiner, J. Sanders and J. Wimmers, "Resolution issues in InSb focal plane array system design, SPIE Proceedings, Infrared FPA Applications, Vol 3377, April 1998.

[2] R. Shannon, "Aberrations and their effects on images, SPIE Proceedings, Geometric Optics, Critical View of Technology, Vol 537, 1885.

[3] G. Holst, Electro-Optical Imaging System Performance, SPIE Optical Enginneering Press, 1995, pp.133.

[4] L.Scott and J. D'Agostino, "NVEOD FLIR92 Thermal Imaging Systems Performance Model, SPIE Proceedings, Infrared Imaging Systems: Design, Analysis, Modeling, and Testing III, April 1992.